Personalized Medicine in Psychiatry xxx (xxxx) xxx–xxx

Contents lists available at ScienceDirect

Personalized Medicine in Psychiatry

journal homepage: www.elsevier.com/locate/pmip

Improving therapy outcome prediction in major depression using multimodal functional neuroimaging: A pilot study

Johannes Schultz[a,b,*], Benjamin Becker[a,b,1], Katrin Preckel[a,b,2], Meike Seifert[a,b], Clemens Mielacher[a,b], Rupert Conrad[c], Alexandra Kleiman[c], Wolfgang Maier[b,d], Keith M. Kendrick[e], René Hurlemann[a,b]

[a] Division of Medical Psychology, University of Bonn, Bonn, Germany
[b] Department of Psychiatry and Psychotherapy, University of Bonn, Bonn, Germany
[c] Department of Psychosomatic Medicine and Psychotherapy, University of Bonn, Bonn, Germany
[d] German Center for Neurodegenerative Diseases (DZNE), Bonn, Germany
[e] Key Laboratory for NeuroInformation, School of Life Science, Center for Information in Medicine, University of Electronic Science and Technology of China, Chengdu, China

ARTICLE INFO

Keywords:
Depression
Classification
Outcome prediction
Emotional face processing
Dorsolateral prefrontal cortex

ABSTRACT

Mounting evidence emphasizes the usefulness of imaging biomarkers for predicting therapy outcome in major depressive disorder (MDD), in particular building on functional imaging studies of task-based responses to emotional face stimuli and resting state-related connectivity patterns. To explore the possibility that prediction accuracy even in small patient samples would significantly gain from integrating data from different imaging modalities, we acquired functional neuroimaging data both at-rest and during exposure to emotional faces from 21 MDD patients before and 7 weeks after treatment-as-usual, as well as from 20 age- and gender-matched control participants assessed at similar intervals. As expected, MDD patients showed disturbed pre-treatment responses to emotional faces, including left amygdala hyperactivation. Therapeutic outcome correlated with pre-treatment activation, with subgenual cingulate response to emotional faces yielding best results (*r* values ranging from 0.4 to 0.66). A support vector machine classifier trained on task-based or resting-state data predicted responder status, with the right dorsolateral prefrontal cortex connectivity pattern yielding best accuracy (88.9%). Crucially, combining task-based with resting-state data increased prediction accuracy by 6.5–7.7 percentage points on average. From this pilot study, we conclude that multimodal functional imaging has the potential of improving therapy outcome prediction even in small MDD sample sizes, resulting in about one additional correct classification every 15 patients. The present results inform future studies which are needed to consolidate imaging approaches as a means of establishing precision medicine in psychiatry.

1. Introduction

Major depressive disorder (MDD) is one of the most common psychiatric conditions, currently the leading cause of disability in the US for people 15–44 years old (1), and predicted to be among the 21st century's most burdensome diseases [1,2]. As remission of depressive symptoms occurs in only one-third of MDD patients after the first antidepressant trial and unsuccessful treatments prolong suffering, development of predictive biomarkers of therapeutic outcome is at the center-stage of current psychiatry research [3–6]. Thanks to its increasing availability in university hospitals, functional neuroimaging is a promising tool in that endeavor [3,7–9], with methodological advances moving towards personalized treatments based on direct pre-treatment measures of neural and behavioral response in MDD [4].

Current neurocircuitry models of MDD emphasize disturbed functional connectivity of frontostriatal and limbic regions [10–16], with deficient emotion regulation functionality assumed to lie at the core of the pathophysiology of MDD [3]. Emotion regulation engages, among other regions, the amygdala and divisions of the medial prefrontal cortex (mPFC), in particular the subgenual part of the anterior cingulate

* Corresponding author at: Medical Psychology Division, University Clinic Bonn, Sigmund-Freud-Str. 25, 53105 Bonn, Germany.
E-mail address: Johannes.Schultz@ukbonn.de (J. Schultz).
[1] Present address: Key Laboratory for NeuroInformation, School of Life Science, Center for Information in Medicine, University of Electronic Science and Technology of China, Chengdu, China.
[2] Present address: Max Planck Institute for Human Cognitive and Brain Sciences, Department of Social Neuroscience, Leipzig, Germany.

https://doi.org/10.1016/j.pmip.2018.09.001
Received 28 July 2018; Received in revised form 3 September 2018; Accepted 12 September 2018

cortex (sgACC) [10,11,13,15,17–19]. The amygdala is a primary hub for early (< 100 ms) assessment of social and emotional stimuli [20–23], and patients with MDD consistently exhibit reduced top-down regulatory interactions between mPFC and amygdala, resulting in increased amygdala responses to negative stimuli [12,24,25]. In particular, the processing of emotional faces [12,21,22] reliably shows activation abnormalities in patients with MDD [26] while controlling for higher-order cognitive processing. In addition, there is accruing evidence that amygdala responses to emotional face stimuli inform treatment outcome prediction in MDD [7,8,27]. Another informative brain region in this regard is the aforementioned sgACC, which contributes to automatic behavioral control and recognition of emotional states, reciprocally communicates with the amygdala, and shows abnormal responses and connectivity signatures in MDD patients [3,10,11,13,15,19,26,28–30]. sgACC pre-treatment hyperactivity normalizes after cognitive, pharmacological and electric stimulation therapy [13,31–33], and is predictive of therapy outcome [11,17,34–37]: the greater the sgACC pre-treatment response to emotional faces (particularly negative emotions), the greater the likelihood of improvement resulting from pharmaco- or psychotherapy [3,8].

In contrast to task-based neuroimaging, resting-state paradigms allow to investigate at the same time multiple distributed areas that seem to be functionally and anatomically connected, including the default mode network (DMN), the dorsal attention network (DAN), the executive control network (ECN), and the salience network (SN) [38–40]. Advantageously for investigations of MDD, resting-state connectivity is less susceptible to the confounding influence of task-relevant cognitive impairments typical of MDD than task-based paradigms. Several networks show altered resting-state signatures in MDD [3,9,15,41–43], with a recent study of over a thousand MDD patients identifying four distinct neurophysiological subtypes defined by specific patterns of dysconnectivity in limbic and frontostriatal circuits [16]. Notably, those patterns were predictive of the response to transcranial magnetic stimulation (TMS) [16]; similarly, another study revealed that connectivity between nodes of the SN and the DMN was predictive of the outcome of psychotherapy [9].

1.1. Aims of the study

The aims of this pilot study were (1) to replicate previous findings relating brain responses to disease severity and treatment outcome using correlation approaches [11,17,34–37] and (2) to explore the possibility that combining data from multiple neuroimaging modalities (namely, task-based and resting-state data) has the potential of improving classification-based therapeutic outcome prediction in MDD [3].

2. Material and methods

2.1. Participants

Functional imaging data were obtained pre- and post-treatment (7-weeks intervals on average) from 21 patients with MDD, and at comparable intervals from 20 age- and sex-matched healthy participants (Table 1). Patients were recruited from August 5, 2013, to January 9, 2015. All patients met DSM-IV criteria for unipolar major depressive disorder (MDD), diagnosed by structured clinical interview for DSM IV [44] conducted by specialist physicians of the University Medical Center in Bonn, and were under treatment according to current guidelines for MDD for the duration of the present study (56) and received selective serotonin reuptake inhibitors (N = 11), Alpha2-receptor-antagonists (N = 6), atypical antipsychotics (N = 5), and group behavioral therapy (N = 16). Exclusion criteria for patients were suicidal ideation, psychotic symptoms and MRI contraindications; for healthy participants, exclusion criteria were any lifetime axis I or II psychiatric disorder and any past or current psychoactive medication.

Table 1
Demographics of participants and clinical scores. Column p indicates p values of a chi-square test (sex) or two-sample t-tests comparing values in patients and controls, or, for "Improvement" data, comparing patients' pre-treatment vs. post-treatment values.

	MDD N = 21		Controls N = 20		p
	Mean (SD)	Range	Mean (SD)	Range	
Sex (M/F)	14/7	–	11/9	–	0.44
Age (years)	37.5 (13.5)	19–62	37.4 (13.7)	19–59	0.92
Education (years)	15.2 (2.8)	11–22	16.4 (2.6)	13–23	0.20
N major episodes	2.82 (2.6)	0–10	0	0	–
Duration of current episode (months)	10.8 (12.2)	1–48	–	–	–
T1-T2 interval (days)	46.8 (9.6)	33–63	53.1 (17.3)	39–70	0.23
Pre-treatment BDI	31.8 (10.2)	9–54	2.8 (3.2)	0–10	< 0.001
Post-treatment BDI	19 (11.6)	2–39	–	–	–
Improvement BDI	38.1% (35.5)	−44 to 95	–	–	< 0.001
Pre-treatment HAMD	19.4 (8.7)	8–44	0.7 (1.1)	0–4	< 0.001
Post-treatment HAMD	10.9 (5.6)	2–25	–	–	
Improvement HAMD	35.0% (43.8)	−100 to 89	–	–	< 0.001

This study was conducted according to the principles of the Declaration of Helsinki 2008 and approved by the local Institutional Review Board (IRB). In accordance with the guidelines of the ethics committee, the study procedures were fully explained prior to the participants providing written informed consent.

2.2. Criteria for response

Study outcome used for the correlation analyses was % change in Beck's Depression Index (BDI) (58) as a result of treatment, and study outcome used for classification analyses was treatment response, defined as a ≥50% decrease from the baseline BDI scores.

2.3. Task-based fMRI experimental paradigm

We employed short-duration presentation of emotional faces, a paradigm previously used in several MDD studies [7,12,24,45]. Stimuli consisted in pictures of faces expressing fear, anger, sadness, disgust, happiness, and no emotion (neutral), selected from the Karolinska Directed Emotional Faces [46]. These stimuli were presented near the threshold of conscious awareness by presenting an emotional face picture very briefly (33 ms), followed immediately by a neutral face picture from the same actor presented for 800 ms. Individual characteristics (e.g. hair) were covered using a mask with the same colour as the background, leaving an oval aperture for the facial features. The inter-stimulus interval varied between 5.5 and 7.5 s (uniform distribution). In each fMRI run, nine stimuli were presented for each emotion in an event-related design; participants underwent 4 runs of about 6 min duration each. Previous psychophysical tests have shown that with this presentation schedule, emotional faces are close to or below the subliminal threshold for discrimination according to signal detection criteria, i.e. most individual participants cannot detect the emotional face stimulus nor discriminate the facial expression [47]. As the aim of this experiment was to measure the response in emotion-related brain regions to emotional face stimuli, participants were asked to report the gender of the face stimuli, a task that focused their attention on the face but was irrelevant to the research question. Stimulus presentation and response collection was implemented using Presentation software (Neurobehavioral Systems, Albany, CA), liquid crystal display video

goggles (Nordic NeuroLab, Bergen, Norway) and a custom MRI-compatible response box.

In line with previous studies [21], participants were asked after the experiment whether they had noticed any abnormalities about the face stimuli presented, to ensure that the emotional faces presented were below the subjective level of awareness. These interviews revealed that 3 patients and 2 control participants had, in some trials, perceived 2 faces presented in rapid succession, one of which displayed an emotion. To ascertain that these participants did not drive the reported effects, we repeated the analysis after omitting these participants' data but observed no substantial changes in the results. In order to evaluate if the information perceived during the task was sufficient for recognition of the presented emotions, a sample of 12 patients repeated the experiment after the fMRI scan at measurement time 2 (i.e. post-treatment or equivalent) and attempted to categorize the face stimuli into six categories (five emotions plus neutral; i.e., a six-alternative forced choice task). Classification performance was not different from chance (mean % correct: 17.5; standard deviation: 3.4; *t*-test vs. chance: $t(11) = 0.85$, $p = 0.41$), indicating that the masking procedure prohibited conscious emotion recognition.

2.4. MRI data acquisition

MRI data were acquired using a 1.5 Tesla Avanto MRI system (Siemens, Erlangen, Germany) equipped with a 12-channel standard head coil at the Life & Brain Centre, Bonn. Imaging data were collected for each participant and measurement point (pre- and post-treatment for participants with MDD, and at similar time intervals for control participants), and consisted in four task-based runs with 119–127 functional images each and one resting-state run (5.75 min, 115 volumes, eyes closed) obtained using a $T2^*$-weighted gradient-echo planar image (EPI) sequence (voxel size = 3 × 3 × 3 mm; TR = 3000 ms; TE = 45 ms; flip angle = 90°; FoV = 192 mm; matrix size = 64 × 64; 35 slices; interleaved slice order with interslice gap of 1 mm). Slices were oriented parallel to the intercommissural plane (AC-PC line). Subsequently, a high-resolution structural image was acquired using a T1-weighted 3D MRI sequence (voxel size = 1 × 1 × 1 mm; TR = 1660 ms; TE = 3.09 ms; flip angle = 15°; matrix size = 256 × 256, no interslice gap). Participants wore earplugs and foam padding was used to reduce head motion.

2.5. Task-based fMRI data analysis

The fMRI data were preprocessed and processed using SPM12 software from the Wellcome Trust Centre for Neuroimaging (www.fil.ion.ucl.ac.uk/spm) running in MATLAB R2015A (The MathWorks, Natick, MA). Preprocessing followed standard procedures as in our previous studies [48]. In brief, after discarding the first 5 images to ascertain that T1-equilibration artefacts were eliminated from the time-series, images were motion-corrected using realignment, the anatomical T1 image was co-registered with the aligned functional images, spatially normalized to the Montreal Neurological Institute (MNI) standard space using a two-step procedure including segmentation of the T1-image and application of the resulting transformation parameters to the functional time-series, resampled at a 3 × 3 × 3 mm resolution, and finally smoothed by convolution with a 8-mm full width at half maximum 3D Gaussian kernel [49]. Preprocessed fMRI data were analyzed using the general linear model (GLM) framework implemented in SPM12, following a 2-step mixed-effects analysis, as is common in SPM for group analyses [50]. The first step used a fixed-effects model to analyze individual data sets, and the second step used a random-effects model to analyze the group aggregate of individual results, described under "whole-brain analysis", below. For the fixed-effects model, a temporal high-pass filter with a cutoff of 128 s was used to remove low-frequency signal drifts and an autoregressive model (AR 1 + white noise) was used to estimate serial correlations in the data. A masking threshold level of 0.2 was used to determine voxel inclusion in the analysis. Following that, a linear combination of regressors in a design matrix was fitted to the task-based data to produce beta estimates [51], which represent the contribution of a particular regressor to the data. The GLM applied to the individual data sets contained separate regressors of interest for each experimental condition (i.e. faces expressing fear, anger, sadness, disgust, happiness and no emotion). These regressors were created by modeling the onset and duration of each stimulus as a series of delta functions representing probable neural events, this time-series was then convolved with the canonical hemodynamic response function (HRF, implemented as a sum of 2 gamma functions in SPM12) to yield predictions of changes in BOLD signal evoked by the stimuli. The design matrix further included a constant term, and 6 realignment parameters (yaw, pitch, and roll and X-, Y-, and Z-axis translation terms, obtained during motion correction) used to model movement-related artefacts not eliminated during realignment (e.g., spin-history effects). 3D parameter estimate maps for each of our experimental conditions (i.e. faces expressing fear, anger, sadness, disgust, happiness and no emotion) were produced for each participant and measurement session (i.e. one per scanning day) and used to calculate contrast maps (see second-level analyses, below).

2.6. Resting-state fMRI data analysis

Resting-state data were analysed using the CONN toolbox for SPM (68), including default preprocessing settings such as slice-time correction, unwarping, denoising using a band-pass filter [0.008–0.09 Hz] and smoothing with a 8-mm full width at half maximum 3D Gaussian kernel. We ran both whole-brain correlation analyses using regions-of-interest (ROIs; see below) as seeds, and seed-to-seed correlation analyses for each subject and measurement point. Seeds were anatomically-defined ROIs relevant in the pathophysiology of depression. They included left and right subgenual cingulate (sgACC, Brodmann Area 25) and left and right amygdala (entire Amygdala, defined using the Anatomy toolbox version 2.1 [52,53]), as well as several regions identified in analyses of the brain at rest, identified using 5 mm-diameter spheres centered on coordinates previously published and used in an MDD study [9,40]: left and right intraparietal sulcus (MNI coordinates: [−41 −39 45; 44 −39 45], part of the dorsal attention network = DAN), left and right dorsolateral prefrontal cortex ([−32 45 30; 32 45 30], executive control network = ECN), left and right anterior insula and dorsal anterior cingulate cortex ([−41 3 6; 41 3 6; 0 21 36], salience network = SN), medial prefrontal cortex and precuneus ([−1 54 27; 0 −52 27], default-mode network = DMN). Whole-brain correlation maps were Fischer-Z transformed, compared across participant groups and measurements, and used in correlation analyses with disease severity or treatment effects. Seed-to-seed data were compared across participant groups and measurements and used in correlation analyses with disease severity or treatment effects and for patient classification analyses.

2.7. Whole-brain group (second-level) analysis

Single-subject parameter maps (task-based data) or Fischer-transformed correlation maps (resting state data) of MDD participants MDD and controls, for both measurement points, were smoothed with a Gaussian kernel imported separately into SPM12's full-factorial analysis of variance (ANOVA) model to evaluate group statistics (second-level analysis; random effects). For task-based data, effects assessed in each voxel of the brain were the response to emotional faces overall (all emotions vs. neutral), and the response to each type of emotional face (i.e. fear, anger, sadness, disgust, happiness each contrasted with neutral) assessed within regions showing differences in the response to emotional faces overall. For the resting-state data, we assessed the connectivity between each seed region and the whole brain. SPM12 uses the Greenhouse–Geisser correction for nonsphericity in the data.

The results were controlled for multiple comparisons by using a whole-brain, voxel-wise family-wise error correction (pFWE = 0.05). Locations of peak activation were defined using MNI coordinates.

2.8. Region-of-interest analysis of task-based fMRI data

We further analysed task-based responses in bilateral amygdalae and subgenual cingulate regions (anatomically-defined, see resting-state analysis above). Parameter estimates for each ROI were extracted from all voxels included in the GLM analysis and averaged across voxels. Parameter estimates in clusters that showed hyper- or hypo-activation in response to emotional faces in patients vs. controls (see Results) were extracted and processed in the same fashion. The resulting summary parameter estimates were then compared across conditions, participant groups and measurements and used in correlation and classifier analyses. ROIs were identical across all participants.

2.9. Treatment outcome prediction: classification procedure

To predict responder status (responder/non-responder) we employed libsvm [54] (available at http://www.csie.ntu.edu.tw/~cjlin/libsvm), a commonly-used implementation of a support vector machine (SVM) run within MATLAB R2015A on a MacPro (late 2013 model) 3.7 GHz Quad-Core Intel Xeon E5 with 64 GB 1866 MHz DDR3 RAM. The type of SVM used was C-SVM.

Features were, for the task-based data, the parameter estimates ("Beta" values calculated in SPM) of the response to each kind of emotional face, averaged across voxels of each ROI, and for the resting-state data, the connectivity (r) values obtained between a given ROI and the other ROIs of interest. The reason for evaluating responses to emotions separately in the task-based data and evaluating connectivity profiles separately by ROI for the resting-state data is that for task-based data neural responses to different emotions were found to be differently predictive of treatment outcome in previous work and combining task-based data across ROI yielded robust classification findings, while many ROIs were candidates for connectivity changes between patients and controls based on the resting-state data. All features were normalised to values between 0 and 1. There was no missing data.

Parameters were either at default values (free parameter of the Gaussian radial basis function g = 1/number of features; tolerance of termination criterion = 0.001) or were systematically assessed: the parameter for the soft margin cost function C was varied (values of 1, 2, 3, 5, 10 and 20 were tested), and 4 kernel types (linear, polynomial, radial basis function, sigmoid) were tested. At this optimization stage, all resulting combinations of kernel and C value were tested in a grid search, performance values (raw accuracy) for all conditions of each modality (task-based or resting-state) were averaged, and the combination yielding the highest average performance was identified: polynomial kernel with C = 1. This kernel and C = 1 were then used to compare classifier performance across conditions and data types. Classifier performance was evaluated using a leave-one-patient-out cross-validation scheme: data from all but one patient were used to train the classifier (labels were responder and non-responder), and correct categorization (as responder or non-responder) of the patient not used during training by the trained classifier was considered a correct response. This procedure was repeated N times, where N = number of patients, yielding a classification accuracy score (N correct classifications/N patients). Significance of the classification accuracy score in each condition was assessed using permutation statistics [55,56]: the actual accuracy scores were compared to a reference distribution of accuracy values observed under the null hypothesis that the data features had no systematic relation to the patient's responder status. This distribution was built by repeating the leave-one-patient-out cross-validation scheme described above 10'000 times, each time shuffling the patients' labels (responder or non-responder) anew during classifier training. The *p*-value of a classification accuracy score was then the fraction of the distribution of accuracy values under the null hypothesis that was greater than, or equal to, the accuracy score actually observed using the correct labels. *P* values resulting from this procedure were corrected for multiple comparisons across conditions using the Holm-Bonferroni procedure [57].

3. Results

3.1. Treatment response

Changes in BDI and HAMD scores in patients as a result of treatment are presented in Table 1. We found a significant decline from pre-treatment to post-treatment, a clinically meaningful response [58]. Out of our 21 patients, there were 7 responders based on BDI criteria.

3.2. Task-based hyper- and deactivations in patients pre-treatment

One cortical brain region showed higher activity during the presentation of emotional faces (contrast: all emotions > neutral faces) in patients pre-treatment (compared to both patients post-treatment and controls; conjunction contrast): the right postcentral gyrus [MNI coordinates: 50–22 60; $Z = 4.84$; cluster size 689 voxels/12 voxels survived voxel-wise $p < 0.05$ FWE threshold]. Cortical brain regions with lower activity in patients pre-treatment (compared to both patients post-treatment and controls) were left inferior frontal gyrus [−36 21 12; $Z = 5.72$; 70/15 voxels], two locations in left middle frontal gyrus [−42 18 42; $Z = 5.62$; 152/31 voxels and −30 30 34; $Z = 4.7$; 86/2 voxels], precuneus [−8 −54 52; $Z = 4.7$; 204/2 voxels], and right posterior middle temporal sulcus [50–50 2; $Z = 4.77$; 80/2 voxels]. These results are shown in Fig. 1A.

3.3. BOLD response to emotional faces in amygdala and subgenual cingulate ROIs

As expected, we found an increased response to emotional compared to neutral faces in the left amygdala in MDD at T1 compared with controls, which normalized after therapy (3-way ANOVA with factors measurement timepoint, subject type and emotion; interaction between measurement timepoint and subject type: $F(1,189) = 11.80$, $p < 0.001$; Fig. 1B). There was no significant effect of emotion or interaction between emotion and subject type or measurement point. Activation in subgenual cingulate cortex (sgACC) did not significantly vary with subject type, measurement timepoint or emotions.

3.4. Correlations between BOLD response to emotional faces and pre-treatment disease severity or treatment outcome

Next, we examined whether the BOLD signal in regions showing abnormal responses to emotional faces in patients and in the anatomically-defined amygdala and subgenual cingulate regions correlated with disease severity and therapy response in patients. The aim of this analysis was to replicate previous similar findings [11,17,34–37]. While correlations between disease severity and activation were not significant, we did find significant correlations between the effects of therapy (% BDI change) and pre-therapy activations in several ROIs (Table 2). Interestingly, different regions showed significant correlations depending on the BOLD contrast used, as follows. Using the BOLD response to neutral faces, we found significant positive correlations in left IFG and precuneus, and negative correlations in right postcentral gyrus and right amygdala; using the BOLD response to the emotional faces, we found significant positive correlations in precuneus for sad faces only. None of these correlations survived correction for multiple comparisons, in contrast to the strong positive correlations we obtained with bilateral subgenual cingulate regions' responses to all emotions. When we subtracted the response to neutral faces from the response to

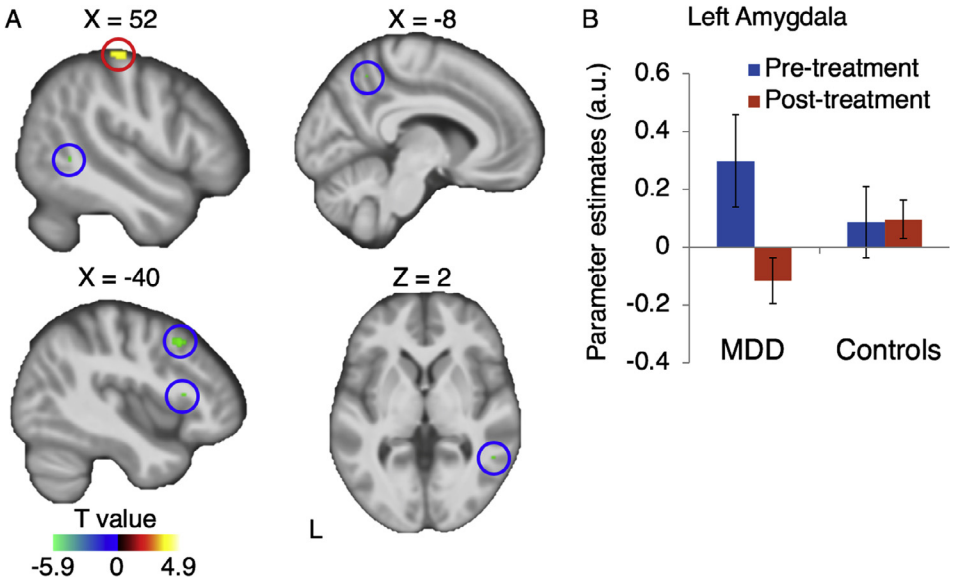

Fig. 1. Abnormal neural response to emotional faces in MDD. A: left inferior and middle frontal gyrus, precuneus and right posterior middle temporal sulcus show decreased (green, blue circles) and right postcentral gyrus shows increased (yellow, red circles) BOLD responses during presentation of emotional faces compared to neutral faces, in patients pre-treatment compared to both patients post-treatment and controls (conjunction contrast). Results are shown here rendered on the average structural scan of all participants, and are thresholded at $p < 0.05$ corrected for family-wise errors (FWE) resulting from multiple comparisons across all voxels of the brain. X and Z values indicate the position of the slice in MNI coordinate space. B: Left amygdala showed an increased response to emotional compared to neutral faces in MDD pre-treatment compared with controls; this response decreased after therapy. (For interpretation of the references to colour in this figure legend, the reader is referred to the web version of this article.)

Table 2
Variance in BDI change (range: 0–1) explained by activation in amygdalae, subgenual cingulate cortex and clusters showing abnormal response to the emotional faces in patients, as a function of the emotion of the face presented. MFG = middle frontal gyrus; DLPFC = dorsolateral prefrontal cortex; IFG = inferior frontal gyrus; pMTG = posterior middle temporal gyrus; sgACC = subgenual anterior cingulate cortex. * = $p < 0.05$ (uncorrected), ** = $p < 0.05$ (Holm-Bonferroni-corrected). Values in italic indicate a negative correlation. Correlations were calculated either using the response evoked by each kind of face stimuli (top half), or after subtracting the response evoked by neutral face stimuli from the response evoked by emotional faces (bottom half).

Correlations between activation and clinical improvement						
Activation evoked by each kind of face						
	Neutral	Angry	Disgusted	Fearful	Happy	Sad
MFG left	0.15	0.01	0.08	0	0.02	0.08
DLPFC left	0.06	*0.01*	0.00	*0.10*	*0.01*	*0.04*
IFG left	0.39*	0.13	0.21	0.03	0.21	0.06
pMTG right	0.16	*0.05*	*0.03*	0	0.01	0
Precuneus	0.42*	0.26	0.13	0.02	0.25	0.26*
Postcentral right	*0.29**	0.08	0	*0.04*	*0.12*	0.04
Amygdala left	*0.25*	0.06	*0.02*	0	0.06	0.03
Amygdala right	*0.29**	0.02	*0.12*	*0.05*	0.01	0
sgACC left	0	0.43*	0.53**	0.66**	0.59**	0.59**
sgACC right	0	0.40*	0.45*	0.61**	0.65**	0.53**
Activation difference between each kind of emotional face and the neutral face						
		Angry	Disgusted	Fearful	Happy	Sad
MFG left	–	*0.30**	*0.16*	*0.42**	*0.27**	*0.14*
DLPFC left	–	*0.17*	*0.19*	*0.29**	*0.17*	*0.28**
IFG left	–	*0.40**	*0.33**	*0.29**	*0.13*	*0.23*
pMTG right	–	*0.37**	*0.51***	*0.25*	*0.15*	*0.32**
Precuneus	–	*0.23*	*0.30**	*0.48***	*0.10*	*0.05*
Postcentral right	–	0.23	0.30*	0.12	0.06	0.24
Amygdala left	–	0.58**	0.17	0.63**	0.49**	0.43*
Amygdala right	–	0.53**	0	0.04	0.31*	0.17
sgACC left	–	0.34*	0.19	0.25	0.38*	0.31*
sgACC right	–	0.23	0.11	0.23	0.40*	0.29

emotional faces, we found negative correlations for one or more emotions in all regions we investigated (of which only two survived corrections for multiple comparisons), except in the amygdala and subgenual cingulate regions. In the amygdala, we found strong positive correlations for several emotions, many of which survived correction for multiple tests, while in the subgenual cingulate, we found positive correlations for several emotions that did not survive multiple comparisons (Table 2).

3.5. Functional connectivity based on resting-state data

A whole-brain search for correlations between resting-state activity in our regions of interest for connectivity analyses and all voxels of the brain revealed that compared with healthy controls, patients showed before treatment a reduced connectivity between the right subgenual cingulate (sgACC) and the right middle frontal gyrus [54 20 14; $Z = 4.86$; cluster size 25 voxels] (Fig. 2). However, in the conjunction contrast comparing patients pre-treatment to both patients post-treatment and controls, no significant results were found. There was no significant correlation between BDI or change in BDI during treatment

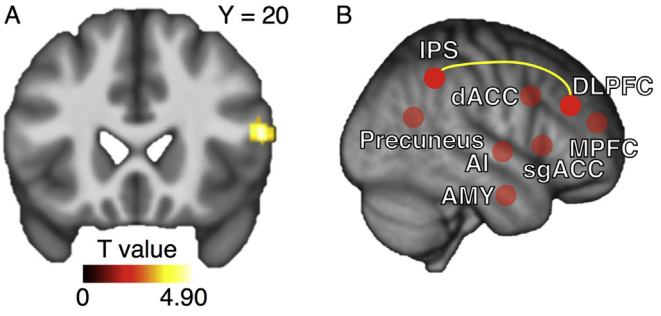

Fig. 2. Results of resting-state functional connectivity analyses. A: Before treatment, patients showed a reduced resting-state functional connectivity between the right subgenual cingulate (sgACC) and the right middle frontal gyrus compared with healthy controls (conventions as in Fig. 1). B: Therapy resulted in a reduction of resting-state connectivity between seeds in right dorsolateral prefrontal cortex and right intraparietal sulcus in patients. Red dots are projections on the right hemispheric surface of the location of connectivity seeds included in the analysis. IPS = intraparietal sulcus; dACC = dorsal anterior cingulate cortex; DLPFC = dorsolateral prefrontal cortex; MPFC = medial prefrontal cortex; AI = anterior insula; sgACC = subgenual anterior cingulate cortex; AMY = amygdala. (For interpretation of the references to colour in this figure legend, the reader is referred to the web version of this article.)

Table 3
Results of a classifier (SVM, see Methods) predicting treatment responder status of one patient based on the task-based and/or resting-state data of the other patients, as a function of the emotion of the face or the seed of the resting-state fMRI connectivity. Values indicate average improvement in percentage points. * = p < 0.05; ** = p < 0.001. P values are corrected for multiple comparisons using the Holm-Bonferroni method. CI = confidence interval. MPFC = medial prefrontal cortex; dACC = dorsal anterior cingulate cortex; AI = anterior insula; DLPFC = dorsolateral prefrontal cortex; IPS = intraparietal sulcus; sgACC = subgenual cingulate.

Name of condition	Accuracy (%)	Accuracy combined with best resting-state data (%)	Improvement % points
Treatment outcome prediction using task-based activation data			
Neutral	66.7	77.8*	11.1**
Angry	72.2	77.8*	5.6
Disgusted	61.1	72.2*	11.1**
Fearful	72.2	72.2*	0
Happy	77.8*	83.3**	5.5
Sad	66.7	72.2*	5.5**
Mean (CI)	69.4 (5.8)	75.9 (4.5)	6.5 (4.2)
Prediction using resting-state connectivity data			
MPFC	44.4	66.7	22.3**
Precuneus	50	66.7	16.7**
dACC	55.6	61.1	5.5**
AI left	50	55.6	5.6**
AI right	61.1	55.6	−5.5
DLPFC left	88.9**	83.3**	−5.6
DLPFC right	77.8	72.2	−5.6
IPS left	83.3*	77.8	−5.5
IPS right	50	72.2	22.2**
Amygdala left	55.6	77.8*	22.2**
Amygdala right	61.1	66.7	5.6*
sgACC left	38.9	55.6	16.7**
sgACC right	50	55.6	5.6*
Mean (CI)	59.0 (15.3)	66.7 (9.6)	7.7 (11.2)

on one hand and connectivity between resting-state activity in our regions of interest and all other regions of the brain on the other hand. Systematic pairwise seed-to-seed correlation analyses between regions of interest revealed that patients' functional connectivity between right DLPFC and right IPS was significantly reduced as a result of therapy ($t(20) = 5.745$, $p_{corr} = 0.01$, 2-sample t-test with Holm-Bonferroni correction for multiple comparisons). There was no difference in seed-to-seed connectivity between patients and controls and no correlation between seed-to-seed connectivity and pre-treatment BDI or change in BDI as a result of treatment.

3.6. Prediction of responder status: comparing classifier performance based on data of one imaging modality or combined across imaging modalities

Finally we addressed the main aim of this study: we assessed whether responder status (i.e. whether a patient responded to treatment or not) could be predicted based on the task-based activations evoked by each emotion (combined activation across ROIs), the resting-state data (pattern of seed-to-seed connectivity for each seed tested), or a combination of task-based and resting-state data. Results (Table 3) show that prediction was indeed possible, that prediction based on task-based data tended to be better (69.4 vs 59% correct, a non-significant difference: $t(17) = 1.60$, $p < 0.13$), and importantly, that supplementing the data of one kind with the best data of the other kind yielded significant improvements of 6.5 percentage points for task-based data ($t(5) = 3.79$, $p < 0.02$) and 7.7 percentage points for resting-state data ($t(12) = 2.47$, $p < 0.03$). Thus, combining imaging modalities yields one additional correct identification every 15 patients.

4. Discussion

The aim of the present pilot study was to explore the potential of combining data from different functional neuroimaging modalities to predict treatment response in MDD. Specifically, we tested the hypothesis that prediction performance could be improved by combining task-based and resting-state neuroimaging data. We replicated previous findings by showing that treatment response can be related to activation differences across patients and could be predicted both from task-based and resting-state data. Crucially, we demonstrate that integrating these two modalities increases prediction accuracy, resulting in about one additional correct classification every 15 patients.

Comparing neural responses in patients pre-treatment against their post-treatment activations as well as against controls, we found increased responses to emotional faces in right postcentral gyrus and the left amygdala, and decreased responses in left inferior and middle frontal gyrus, precuneus, and right posterior middle temporal sulcus. Except for the postcentral gyrus, these regions have all been associated with emotional responses, emotion recognition, and emotion regulation [59], and most have previously been shown to abnormally respond to emotional stimuli in mood disorders [3,26,29]. The effects of therapy correlated very well with the following aspects of these activations: (a) pre-treatment response to neutral faces in precuneus, left inferior frontal gyrus, right amygdala and right parietal cortex; (b) the response to emotional faces in subgenual cingulate; and (c) the differential response to emotional vs. neutral faces in most of these regions. In general, in regions deactivated in patients pre-therapy compared to post-therapy and compared to controls, responses correlated negatively with therapy outcome. Our results thus confirm the vast previous findings indicating that MDD therapy outcomes correlate with neural responses to neutral and emotional stimuli [3,8]. However, our results reveal a contrast between findings in regions responding to emotional faces compared to findings in subgenual cingulate: in the former regions, the highest correlations with therapy outcome were obtained using a differential response (response to emotional faces minus response to neutral faces, thus removing responses to the face per se), and the emotion with best results varied across regions; while in the subgenual cingulate, the response to emotional faces allowed extremely robust prediction results (positive correlations) using the response to each of the emotions (Table 2). The latter finding concords very well with previous reports of subgenual cingulate activity being predictive of therapy outcome [11,17,34–37], in particular with the common finding that greater activity relates to greater improvement [3,8]. Our results are thus in line with previous findings reporting that task-based activation correlates with therapy outcome.

Analysis of the resting-state data revealed reduced connectivity between the right subgenual cingulate and the right middle frontal gyrus in patients compared to controls. This finding is consistent with a large body of literature demonstrating abnormalities in the emotion regulation network in MDD, particularly connectivity between subgenual cingulate and other prefrontal regions [3,10,11,13,15,19,26,28–30]. Further, therapy resulted in reduction of seed-to-seed connectivity between right DLPFC and right IPS in MDD patients. These data confirm previous findings of abnormal seed-to-seed connectivity in MDD [15,41–43], specifically about connectivity between dorsolateral prefrontal and inferior parietal cortex [60], and findings indicating that therapy leads to changes in connectivity [61–63]. While therapy outcome can be predicted from changes in resting-state connectivity [9,16,62], our data have not yielded such results, most probably due to the relatively small sample of patients included in the study.

Using a common Support Vector Machine (SVM) algorithm, we could predict patients' response status with an accuracy of up to 88.9% based on neuroimaging data. Prediction using task-based data was on average 10 percentage points higher than prediction based on resting-state data, but the highest prediction scores were obtained using the

latter. Interestingly, significant prediction from task-based data could be obtained only using the response to happy faces, while significant prediction from resting-state data could be obtained only from the connectivity pattern originating in the left intraparietal sulcus or the left dorsolateral prefrontal cortex. While our analysis is based on a small sample of patients and the classification accuracies we report are thus likely to be inflated [64], our findings suggest that results based on only one kind of neuroimaging data are more variable across patient subsamples than results based on multiple kinds of data. Combining the best-predicting resting-state data with the task-based data significantly improved accuracy, enabling significant prediction using the data of all emotional faces. While the complementary manipulation of combining the best-predicting task-based data with the resting-state data again also significantly improved accuracy overall, the number of seeds yielding significant prediction results was left unchanged (N = 2 seeds), and four seeds even showed decreased accuracy, indicating that the classifier relied on non-informative data features. These results suggest that the best method to achieve significant prediction is to supplement task-based data with the resting-state connectivity pattern of the left dorsolateral prefrontal cortex.

In our present data, clinically important, task-based prediction of therapy outcome could be obtained only using the response to happy faces; with the subgenual cingulate cortex' response to happy faces eliciting the strongest associations with clinical outcome. Differences in the ability to emotionally process positive facial expressions have crucial implications for the therapeutic relationship [65] and the possibility to capitalize on social reinforcements [66], both of which are essential ingredients of depression therapy [67].

We must acknowledge several limitations of our pilot study, which suggest that the preliminary results presented here should be taken with caution. First, the patient sample from which the data where acquired was very small (N = 21), heterogeneous in age, disease severity and duration, outcome, treatment protocol and recruited from only one site. Second, several aspects of the analysis may be optimized in future work. While we used a valid classification procedure relying on simple leave-one-patient-out cross-validation, this approach has recently been shown to yield artificially high accuracies in small samples [64,68]. Notably, as we optimised the parameters and tested the model using the same dataset, higher accuracies may have occurred by chance or through classifier overfitting. Recent developments such as nested cross-validation [69] have demonstrated higher reliability and show great promise for further investigations aiming to uncover the most relevant variables for accurate treatment outcome prediction. Further particularities of our analyses should be mentioned, for example the fact that we did not use the same number of ROIs for the analysis of task-based and resting-state data (comparing accuracies based on the different kinds of data was not an aim of our study), and the fact that using balanced accuracy rather than raw accuracy may be a better option for analysing classes of unequal sizes. The small sample size and these methodological details may be the reason why we observed large variations in prediction accuracy across conditions (task-based: 44.4–88.9%, resting-state-based: 61.1–77.8%). This variation might be due to genuine differences in information content regarding outcome across regions or to noisy data. For this reason, we did not expand too much on the differences across conditions. Our aim was to evaluate if combining modalities improves prediction accuracy irrespective of the number of ROIs contributing to each modality, and we have considered the conditions as that many tests allowing address this question. The results are coherent: accuracy for each modality can be improved by adding data from the other modality.

Another important aspect of this study is that we have only attempted to predict treatment outcome in general and not outcomes for different treatments. This second aspect is necessary to reach the ultimate goal of the present research, which is to provide recommendations for specific treatments for individual patients. Some successes have already been achieved in this direction e.g. [70]. Our present work shows that combining multiple neuroimaging modalities improves outcome prediction; future work combining clinical data and different kinds of neuroimaging data may prove promising in order to identify the best treatment option for each individual.

Regarding the practical value of our approach, we must admit that acquiring MRI data is expensive in comparison to collecting clinical questionnaires. However, MRI scanners are nowadays quite widely available, data analysis is largely user-independent (especially for routine anatomical scans but also for simple functional paradigms), and crucially, the technique measures neurobiological variables rather than subjective mental states. The latter aspect allows to apply the technique even to patients incapable of reliable introspection or affected by mutism due to severe MDD. Future developments in the neuropsychopathology of MDD may provide more precise constraints on the brain regions to consider for outcome prediction, further improving prediction performance. Therefore, despite its costs, we believe that MRI-based outcome prediction is a useful avenue to pursue.

In summary, our study confirms the usefulness of neuroimaging in the prediction of therapy outcome of MDD and the benefits of acquiring several kinds of longitudinal neuroimaging data. Our findings demonstrate that in the prediction of treatment response, task-based and resting-state neuroimaging modalities are complementary rather than redundant [8]. Critically, our findings may inform future studies evaluating if combining neuroimaging data can help to formulate personalized treatment recommendations, thereby minimizing unnecessary treatment and the associated suffering and health care costs. This strategy may be an important step in the process of establishing precision medicine in psychiatry.

Acknowledgements

The authors would like to acknowledge the help of Alexandra Patin for organizing the data and Paul Jung for task programming. This research did not receive any specific grant from funding agencies in the public, commercial, or not-for-profit sectors.

Conflict of interest

The authors declare no conflict of interest.

Appendix A. Supplementary data

Supplementary data to this article can be found online at https://doi.org/10.1016/j.pmip.2018.09.001.

References

[1] Collins PY, Patel V, Joestl SS, March D, Insel TR, Daar AS, et al. Grand challenges in global mental health. Nature 2011;475:27–30. https://doi.org/10.1038/475027a.
[2] Kupfer DJ, Frank E, Phillips ML. Major depressive disorder: new clinical, neurobiological, and treatment perspectives. Lancet 2012;379:1045–55. https://doi.org/10.1016/S0140-6736(11)60602-8.
[3] Phillips ML, Chase HW, Sheline YI, Etkin A, Almeida JRC, Deckersbach T, et al. Identifying predictors,moderators, and mediators of antidepressant response in major depressive disorder. Neuroimaging Approaches 2015;172:124–38. https://doi.org/10.1176/appi.ajp.2014.14010076.
[4] McGrath CL, Kelley ME, Holtzheimer PE, Dunlop BW, Craighead WE, Franco AR, et al. Toward a neuroimaging treatment selection biomarker for major depressive disorder. JAMA Psychiatry 2013;70:821–9. https://doi.org/10.1001/jamapsychiatry.2013.143.
[5] Walter M, Lord A. How can we predict treatment outcome for depression? EBioMed 2015;2:9–10. https://doi.org/10.1016/j.ebiom.2014.12.008.
[6] Hahn T, Nierenberg AA, Whitfield-Gabrieli S. Predictive analytics in mental health: applications, guidelines, challenges and perspectives. Mol Psychiatry 2016;22:37–43. https://doi.org/10.1038/mp.2016.201.
[7] Williams LM, Korgaonkar MS, Song YC, Paton R, Eagles S, Goldstein-Piekarski A, et al. Amygdala reactivity to emotional faces in the prediction of general and medication-specific responses to antidepressant treatment in the randomized iSPOT-D trial. Neuropsychopharmacology 2015;40:2398–408. https://doi.org/10.1038/npp.2015.89.
[8] Fu CHY, Steiner H, Costafreda SG. Predictive neural biomarkers of clinical response

in depression: a meta-analysis of functional and structural neuroimaging studies of pharmacological and psychological therapies. Neurobiol Dis 2013;52:75–83. https://doi.org/10.1016/j.nbd.2012.05.008.
[9] Crowther A, Smoski MJ, Minkel J, Moore T, Gibbs D, Petty C, et al. Resting-state connectivity predictors of response to psychotherapy in major depressive disorder. Neuropsychopharmacology 2015;40:1659–73. https://doi.org/10.1038/npp.2015.12.
[10] Drevets WC, Price JL, Simpson JR, Todd RD, Reich T, Vannier M, et al. Subgenual prefrontal cortex abnormalities in mood disorders. Nature 1997;386:824–7. https://doi.org/10.1038/386824a0.
[11] Mayberg HS, Brannan SK, Mahurin RK, Jerabek PA, Brickman JS, Tekell JL, et al. Cingulate function in depression: a potential predictor of treatment response. NeuroReport 1997;8:1057.
[12] Sheline YI, Barch DM, Donnelly JM, Ollinger JM, Snyder AZ, Mintun MA. Increased amygdala response to masked emotional faces in depressed subjects resolves with antidepressant treatment: an fMRI study. Biol Psychiatry 2001;50:651–8.
[13] Mayberg HS, Lozano AM, Voon V, McNeely HE, Seminowicz D, Hamani C, et al. Deep brain stimulation for treatment-resistant depression. Neuron 2005;45:651–60. https://doi.org/10.1016/j.neuron.2005.02.014.
[14] Pezawas L, Meyer-Lindenberg A, Drabant EM, Verchinski BA, Munoz KE, Kolachana BS, et al. 5-HTTLPR polymorphism impacts human cingulate-amygdala interactions: a genetic susceptibility mechanism for depression. Nat Neurosci 2005;8:828–34. https://doi.org/10.1038/nn1463.
[15] Greicius MD, Flores BH, Menon V, Glover GH, Solvason HB, Kenna H, et al. Resting-state functional connectivity in major depression: abnormally increased contributions from subgenual cingulate cortex and thalamus. Biol Psychiatry 2007;62:429–37. https://doi.org/10.1016/j.biopsych.2006.09.020.
[16] Drysdale AT, Grosenick L, Downar J, Dunlop K, Mansouri F, Meng Y, et al. Resting-state connectivity biomarkers define neurophysiological subtypes of depression. Nat Med 2017;23:28–38. https://doi.org/10.1038/nm.4246.
[17] Siegle G, Siegle GJ, Carter CS, Thase ME. Use of fMRI to predict recovery from unipolar depression with cognitive. Behav Ther 2006;163:735–8. https://doi.org/10.1176/appi.ajp.163.4.735.
[18] Siegle GJ, Thompson WK, Collier A, Berman SR, Feldmiller J, Thase ME, et al. Toward clinically useful neuroimaging in depression treatment. Arch Gen Psychiatry 2012;69:913–24. https://doi.org/10.1001/archgenpsychiatry.2012.65.
[19] Agid Y, Buzsáki G, Diamond DM, Frackowiak RSJ, Giedd J, Girault J-A, et al. How can drug discovery for psychiatric disorders be improved? Nat Rev Drug Discov 2007;6:189–201. https://doi.org/10.1038/nrd2217.
[20] Morris JS, Frith CD, Perrett DI, Rowland D, Young AW, Calder AJ, et al. A differential neural response in the human amygdala to fearful and happy facial expressions. Nature 1996;383:812–5. https://doi.org/10.1038/383812a0.
[21] Whalen PJ, Rauch SL, Etcoff NL, McInerney SC, Lee MB, Jenike MA. Masked presentations of emotional facial expressions modulate amygdala activity without explicit knowledge. J Neurosci 1998;18:411–8.
[22] Morris JS, Ohman A, Dolan RJ. Conscious and unconscious emotional learning in the human amygdala. Nature 1998;393:467–70. https://doi.org/10.1038/30976.
[23] Phelps EA, Ledoux JE. Contributions of the amygdala to emotion processing: from animal models to human behavior. Neuron 2005;48:175–87. https://doi.org/10.1016/j.neuron.2005.09.025.
[24] Suslow T, Konrad C, Kugel H, Rumstadt D, Zwitserlood P, Schöning S, et al. Automatic mood-congruent amygdala responses to masked facial expressions in major depression. Biol Psychiatry 2010;67:155–60. https://doi.org/10.1016/j.biopsych.2009.07.023.
[25] Stuhrmann A, Dohm K, Kugel H, Zwanzger P, Redlich R, Grotegerd D, et al. Mood-congruent amygdala responses to subliminally presented facial expressions in major depression: associations with anhedonia. J Psychiatry Neurosci 2013;38:249–58. https://doi.org/10.1503/jpn.120060.
[26] Stuhrmann A, Suslow T, Dannlowski U. Facial emotion processing in major depression: a systematic review of neuroimaging findings. Biol Mood Anxiety Disord 2011;1:10. https://doi.org/10.1186/2045-5380-1-10.
[27] Canli T, Cooney RE, Goldin P, Shah M, Sivers H, Thomason ME, et al. Amygdala reactivity to emotional faces predicts improvement in major depression. NeuroReport 2005;16:1267.
[28] Ressler KJ, Mayberg HS. Targeting abnormal neural circuits in mood and anxiety disorders: from the laboratory to the clinic. Nat Neurosci 2007;10:1116–24. https://doi.org/10.1038/nn1944.
[29] Drevets WC, Price JL, Furey ML. Brain structural and functional abnormalities in mood disorders: implications for neurocircuitry models of depression. Brain Struct Funct 2008;213:93–118. https://doi.org/10.1007/s00429-008-0189-x.
[30] Phillips ML, Ladouceur CD, Drevets WC. A neural model of voluntary and automatic emotion regulation: implications for understanding the pathophysiology and neurodevelopment of bipolar disorder. Mol Psychiatry 2008;13:833–57. https://doi.org/10.1038/mp.2008.65.
[31] Fu CHY, Williams SCR, Cleare AJ, Brammer MJ, Walsh ND, Kim J, et al. Attenuation of the neural response to sad faces in major depressionby antidepressant treatment. Arch Gen Psychiatry 2004;61:877–89. https://doi.org/10.1001/archpsyc.61.9.877.
[32] Goldapple K, Segal Z, Garson C, Lau M, Bieling P, Kennedy S, et al. Modulation of cortical-limbic pathways in major depression. Arch Gen Psychiatry 2004;61:34–41. https://doi.org/10.1001/archpsyc.61.1.34.
[33] Chen C-H, Ridler K, Suckling J, Williams S, Fu CHY, Merlo-Pich E, et al. Brain imaging correlates of depressive symptom severity and predictors of symptom improvement after antidepressant treatment. Biol Psychiatry 2007;62:407–14. https://doi.org/10.1016/j.biopsych.2006.09.018.
[34] Keedwell PA, Drapier D, Surguladze S, Giampietro V, Brammer M, Phillips M. Subgenual cingulate and visual cortex responses to sad faces predict clinical outcome during antidepressant treatment for depression☆. J Affect Disord 2010;120:120–5. https://doi.org/10.1016/j.jad.2009.04.031.
[35] Salvadore G, Cornwell BR, Colon-Rosario V, Coppola R, Grillon C, Zarate Jr CA, et al. Increased anterior cingulate cortical activity in response to fearful faces: a neurophysiological biomarker that predicts rapid antidepressant response to ketamine. Biol Psychiatry 2009;65:289–95. https://doi.org/10.1016/j.biopsych.2008.08.014.
[36] Fox MD, Buckner RL, White MP, Greicius MD, Pascual-Leone A. Efficacy of transcranial magnetic stimulation targets for depression is related to intrinsic functional connectivity with the subgenual cingulate. Biol Psychiatry 2012;72:595–603. https://doi.org/10.1016/j.biopsych.2012.04.028.
[37] Downar J, Geraci J, Salomons TV, Dunlop K, Wheeler S, McAndrews MP, et al. Anhedonia and reward-circuit connectivity distinguish nonresponders from responders to dorsomedial prefrontal repetitive transcranial magnetic stimulation in major depression. Biol Psychiatry 2014;76:176–85. https://doi.org/10.1016/j.biopsych.2013.10.026.
[38] Fox MD, Snyder AZ, Vincent JL, Corbetta M, Van Essen DC, Raichle ME. The human brain is intrinsically organized into dynamic, anticorrelated functional networks. P Natl Acad Sci USA 2005;102:9673–8. https://doi.org/10.1073/pnas.0504136102.
[39] Fox MD, Raichle ME. Spontaneous fluctuations in brain activity observed with functional magnetic resonance imaging. Nat Rev Neurosci 2007;8:700–11. https://doi.org/10.1038/nrn2201.
[40] Raichle ME. The restless brain. Brain Connec 2011;1:3–12. https://doi.org/10.1089/brain.2011.0019.
[41] Wang L, Hermens DF, Hickie IB, Lagopoulos J. A systematic review of resting-state functional-MRI studies in major depression. J Affect Disord 2012;142:6–12. https://doi.org/10.1016/j.jad.2012.04.013.
[42] Bhaumik R, Jenkins LM, Gowins JR, Jacobs RH, Barba A, Bhaumik DK, et al. Multivariate pattern analysis strategies in detection of remitted major depressive disorder using resting state functional connectivity. NeuroImage: Clinical 2016. https://doi.org/10.1016/j.nicl.2016.02.018.
[43] Sambataro F, Wolf ND, Pennuto M, Vasic N, Wolf RC. Revisiting default mode network function in major depression: evidence for disrupted subsystem connectivity. Psychol Med 2014;44:2041–51. https://doi.org/10.1017/S0033291713002596.
[44] Wittchen HU, Wunderlich U, Gruschwitz S, Zaudig M. SKID I. Strukturiertes Klinisches Interview für DSM-IV. Achse I: Psychische Störungen. Interviewheft und Beurteilungsheft. Eine deutschsprachige, erweiterte Bearb. d. amerikanischen Originalversion des SKID I 1997.
[45] Dannlowski U, Dannlowski U, Kersting A, Kersting A, Donges U-S, Donges US, et al. Masked facial affect priming is associated with therapy response in clinical depression. Eur Arch Psychiatry Clin Neurosci 2005;256:215–21. https://doi.org/10.1007/s00406-005-0628-0.
[46] Lundqvist D, Flykt A, Ohman A. The Karolinska directed emotional faces (KDEF). CD ROM From Department of Clinical Neuroscience, Psychology Section, Karolinska Institutet 1998.
[47] Williams LM, Liddell BJ, Rathjen J, Brown KJ, Gray J, Phillips M, et al. Mapping the time course of nonconscious and conscious perception of fear: an integration of central and peripheral measures. Hum Brain Mapp 2004;21:64–74. https://doi.org/10.1002/hbm.10154.
[48] Schultz J, Brockhaus M, Bülthoff HH, Pilz KS. What the human brain likes about facial motion. Cereb Cortex 2013;23:1167–78. https://doi.org/10.1093/cercor/bhs106.
[49] Friston KJ, Ashburner J, Frith CD, Poline J-B, Heather J, Frackowiak RSJ. Spatial registration and normalisation of images. Hum Brain Mapp 1995;2:165–89.
[50] Friston KJ, Holmes AP, Price CJ, Buchel C, Worsley KJ. Multisubject fMRI studies and conjunction analyses. NeuroImage 1999;10:385–96. https://doi.org/10.1006/nimg.1999.0484.
[51] Friston KJ, Holmes AP, Worsley KJ, Poline JP, Frith CD, Frackowiak RSJ. Statistical parametric maps in functional imaging: a general linear approach. Hum Brain Mapp 1995;2:189–210. https://doi.org/10.1002/hbm.460020402.
[52] Eickhoff SB, Stephan KE, Mohlberg H, Grefkes C, Fink GR, Amunts K, et al. A new SPM toolbox for combining probabilistic cytoarchitectonic maps and functional imaging data. NeuroImage 2005;25:1325–35. https://doi.org/10.1016/j.neuroimage.2004.12.034.
[53] Palomero-Gallagher N, Eickhoff SB, Hoffstaedter F, Schleicher A, Mohlberg H, Vogt BA, et al. Functional organization of human subgenual cortical areas: relationship between architectonical segregation and connectional heterogeneity. NeuroImage 2015;115:177–90. https://doi.org/10.1016/j.neuroimage.2015.04.053.
[54] Chang C-C, Lin C-J. LIBSVM: a library for support vector machines. Acm Tist 2011;2:27–37. https://doi.org/10.1145/1961189.1961199.
[55] Ojala M, Garriga GC. permutation tests for studying classifier performance. J Mach Learn Res 2010;11:1833–63.
[56] Pereira F, Botvinick M. Information mapping with pattern classifiers: a comparative study. NeuroImage 2011;56:476–96. https://doi.org/10.1016/j.neuroimage.2010.05.026.
[57] Holm S. A simple sequentially rejective multiple test procedure. Scand J Stat 1979;6:65–70.
[58] Jacobson NS, Truax P. Clinical significance: a statistical approach to defining meaningful change in psychotherapy research. J Consult Clin Psychol 1991;59:12–9.
[59] Dricu M, Frühholz S. Perceiving emotional expressions in others: activation likelihood estimation meta-analyses of explicit evaluation, passive perception and incidental perception of emotions. Neurosci Biobehav R 2016;71:810–28. https://doi.org/10.1016/j.neubiorev.2016.10.020.
[60] Sheline YI, Price JL, Yan Z, Mintun MA. Resting-state functional MRI in depression

unmasks increased connectivity between networks via the dorsal nexus. P Natl Acad Sci USA 2010;107:11020–5. https://doi.org/10.1073/pnas.1000446107.
[61] Abbott CC, Lemke NT, Gopal S, Thoma RJ, Bustillo J, Calhoun VD, et al. Electroconvulsive therapy response in major depressive disorder: a pilot functional network connectivity resting state fmri investigation. Front Psychiatry 2013;4. https://doi.org/10.3389/fpsyt.2013.00010.
[62] Fu CHY, Costafreda SG, Sankar A, Adams TM, Rasenick MM, Liu P, et al. Multimodal functional and structural neuroimaging investigation of major depressive disorder following treatment with duloxetine. BMC Psychiatry 2015;15:82. https://doi.org/10.1186/s12888-015-0457-2.
[63] Spies M, Kraus C, Geissberger N, Auer B, Klöbl M, Tik M, et al. Default mode network deactivation during emotion processing predicts early antidepressant response. Transl Psychiatry 2017;7:e1008–9. https://doi.org/10.1038/tp.2016.265.
[64] Varoquaux G. Cross-validation failure: small sample sizes lead to large error bars. NeuroImage 2017. https://doi.org/10.1016/j.neuroimage.2017.06.061.
[65] Mikulincer M, Shaver PR. An attachment perspective on psychopathology. World Psychiatry 2012;11:11–5. https://doi.org/10.1002/(ISSN)2051-5545.
[66] Lewinsohn PM, Sullivan JM, Grosscup SJ. Changing reinforcing events: an approach to the treatment of depression. Psychother Theory Res Pract 1980;17:322–34. https://doi.org/10.1037/h0085929.
[67] Lara ME, Klein DN. Psychosocial processes underlying the maintenance and persistence of depression: implications for understanding chronic depression. Clin Psychol Rev 1999;19:553–70.
[68] Woo C-W, Chang LJ, Lindquist MA, Wager TD. Building better biomarkers: brain models in translational neuroimaging. Nat Neurosci 2017;20:365–77. https://doi.org/10.1038/nn.4478.
[69] Koutsouleris N, Kahn RS, Chekroud AM, Leucht S, Falkai P, Wobrock T, et al. Multisite prediction of 4-week and 52-week treatment outcomes in patients with first-episode psychosis: a machine learning approach. Lancet Psychiatry 2016;3:935–46. https://doi.org/10.1016/S2215-0366(16)30171-7.
[70] Chekroud AM, Zotti RJ, Shehzad Z, Gueorguieva R, Johnson MK, Trivedi MH, et al. Cross-trial prediction of treatment outcome in depression: a machine learning approach. Lancet Psychiatry 2016;3:243–50. https://doi.org/10.1016/S2215-0366(15)00471-X.